Predicting phase steps in phase-shifting interferometry in the presence of noise and harmonics

Rajesh Langoju, Abhijit Patil, and Pramod Rastogi

A novel method for estimating pixelwise phase step values in phase-shifting interferometry is presented. The method is based on the linear prediction property of the intensity fringes recorded temporally at a pixel on the charged-coupled device. The salient features of the method lie in their ability to handle linear miscalibration errors, to compensate for the presence of harmonics in an optical configuration and detector nonlinearity, and to allow for the use of arbitrary phase steps. The robustness of the proposed method is studied in the presence of noise and a comparison with several benchmarking algorithms is performed. The simulation results show the efficiency of the algorithm in retrieving the wrapped phase. © 2006 Optical Society of America

OCIS codes: 120.3180, 120.5050.

1. Introduction

Phase shifting[1–15] is a topic of interest in optical interferometry because of its ability to bring automation in its fold. The technique functions by recording N frames of intensity data shifted in phase with respect to each other. The phase shifts are provided by a piezoelectric actuator (PZT). The set of intensity equations at each pixel is solved to compute the phase. However, the measurement is prone to errors. One of the most common sources of errors in phase evaluation arises from the inaccurate calibration of the PZT. Factors such as the aging of the PZT, hysteresis, and environmental changes only contribute to aggravating the problem. Phase measurement is also sensitive to the nonlinearity of the detector and multiple beam interference (a consequence of multiple reflections in a laser cavity).[13–15] Algorithms have been proposed to compensate for some of these error sources. For example, the algorithm developed in Ref. 1, though suitable for compensating for first-order calibration errors of the PZT, would need a careful selection of phase steps for optimum operation, and whereas the algorithms proposed in Refs. 12 and 15 minimize the linear calibration errors in PZT, the algorithm proposed in Ref. 14 offers the possibility to reduce the calibration error in the presence of higher-order harmonics. References 13 and 14 show that κth order harmonic can be minimized with phase steps of $2\pi/(\kappa + 2)$ between acquired data frames.

The objective of this paper is to propose what is believed to be a novel approach for obtaining phase measurement in the presence of PZT miscalibration and multiple-order harmonics in the sampled waveform. The method, by enabling us to freely choose phase shifts between 0 and π rad, completely avoids imposing conditions on the phase shift that must be applied. The selection of arbitrary phase steps is obtained by exploiting the linear prediction property[16] of the intensity fringes recorded temporally at the (x, y) pixel of the N data frames. The method basically explores the fact that the intensity at any pixel (x, y) at the nth instant can be predicted from the previous 2κ data frames in which κ is the number of harmonics present in the intensity fringes. This prediction of intensity at any instant for a data frame is related to its past 2κ data frames by constants commonly known as coefficients. The determination of these coefficients allows for the retrieval of phase steps at each pixel point. The number of data samples required for estimating the phase steps in the presence of the κth-order harmonic is $4\kappa + 1$. The phase step values at each pixel being known, the phase distribution can be computed pixelwise by solving the linear Vandermonde system of equations or by using the generalized approach suggested by Morgan[17] and Grievenkamp.[18] Since the phase steps are estimated

The authors are with the Applied Computing and Mechanics Laboratory, Ecole Polytechnique Fédérale de Lausanne, 1015 Lausanne, Switzerland. P. Rastogi's e-mail address is pramod.rastogi@epfl.ch.

Received 14 October 2005; revised 18 March 2006; accepted 20 March 2006; posted 21 March 2006 (Doc. ID 65365).

0003-6935/06/246106-07$15.00/0

pixelwise, the proposed method has the potential to work efficiently with both diverging and converging beams. The robustness of the proposed method is tested by introducing additive white Gaussian noise[19] during the estimation of the phase step values.

2. Linear Prediction Approach

A simple mathematical representation of the recorded interference fringe intensity at a pixel (x, y) for κth harmonic and over N data frames is

$$I_n(x, y) = I_0(x, y)\Big(1 + \sum_{k=1}^{\kappa} \gamma_k(x, y) \times \cos\{k[n\alpha(x, y) + \varphi(x, y)]\}\Big), \quad n = 0, 1, 2, \ldots, N-1, \tag{1}$$

where I_0, γ_k, φ, and α represent the local background intensity, the fringe visibility of the kth harmonic, the phase distribution randomly distributed between $[0, 2\pi)$, and the phase shift, respectively, on the nth data frame.

A problem commonly faced while evaluating phase φ from N phase-shifted interferograms resides in the miscalibration of the PZTs. A possible solution for minimizing this error source consists of computing the phase steps pixelwise rather than relying on the previously calibrated phase-shifted values. These phase step values could then be used for the computation of the interference phase distribution. The objective of this section is to provide a means for predicting the phase step values pixelwise in the presence of noise. Let us write the difference between the two consecutive data frames in Eq. (1):

$$\begin{aligned}\bar{I}_n(x, y) &= I_{n+1}(x, y) - I_n(x, y), \quad n = 0, 1, 2, 3, \ldots, N-2 \\ &= -2I_{\mathrm{dc}}(x, y)\sum_{k=1}^{\kappa} \gamma_k(x, y) \times \sin\left\{k\left[\left(n + \frac{1}{2}\right)\alpha(x, y) + \varphi(x, y)\right]\right\} \times \sin\left(\frac{k\alpha}{2}\right) \\ &= -2I_{\mathrm{dc}}(x, y)\sum_{k=1}^{\kappa} \gamma_k(x, y) \times \sin\{k[n\alpha(x, y) + \phi(x, y)]\} \times \sin\left(\frac{k\alpha}{2}\right) \\ &= \sum_{k=1}^{\kappa} A_k \sin\{k[n\alpha(x, y) + \phi(x, y)]\},\end{aligned} \tag{2}$$

where $A_k = -2\gamma_k(x, y)I_{\mathrm{dc}}(x, y)\sin(k\alpha/2)$ and $\phi(x, y) = \alpha(x, y)/2 + \varphi(x, y)$.

Let us form a signal D_n consisting of a linear combination of past 2κ values of $\bar{I}_n$ and express it as

$$\begin{aligned}D_n &= a_1\bar{I}_{n-1} + a_2\bar{I}_{n-2} + \cdots + a_{2\kappa-1}\bar{I}_{n-2\kappa+1} + a_{2\kappa}\bar{I}_{n-2\kappa} \\ &= a_1\sum_{k=1}^{\kappa} A_k \sin\{k[(n-1)\alpha + \phi]\} + a_2\sum_{k=1}^{\kappa} A_k \sin\{k[(n-2)\alpha + \phi]\} + \cdots \\ &\quad + a_{2\kappa-1}\sum_{k=1}^{\kappa} A_k \sin\{k[(n-2\kappa+1)\alpha + \phi]\} + a_{2\kappa}\sum_{k=1}^{\kappa} A_k \sin\{k[(n-2\kappa)\alpha + \phi]\} \\ &= \sum_{l=1}^{2\kappa} a_l \sum_{k=1}^{\kappa} A_k \sin\{k[(n-1)\alpha + \phi]\},\end{aligned} \tag{3}$$

where $\{a_l\}$ are the set of linear coefficients. Expanding the right-hand side of Eq. (3) yields

$$D_n = \sum_{k=1}^{\kappa} A_k \sin[k(n\alpha + \phi)]\sum_{l=1}^{2\kappa} a_l \cos(kl\alpha) - \sum_{k=1}^{\kappa} A_k \cos[k(n\alpha + \phi)]\sum_{l=1}^{2\kappa} a_l \sin(kl\alpha). \tag{4}$$

Note that Eqs. (2) and (4) are similar, provided that

$$\sum_{l=1}^{2\kappa} a_l \cos(kl\alpha) = 1, \qquad \sum_{l=1}^{2\kappa} a_l \sin(kl\alpha) = 0. \tag{5}$$

From Eq. (5) we can deduce that

$$1 - \sum_{l=1}^{2\kappa} a_l \exp(-j\omega l)\big|_{\omega=k\alpha} = 0. \tag{6}$$

Provided that the phase step value α and all the k harmonics satisfy Eq. (6) with a set of linear coefficients $\{a_l\}$, then in this case the intensity value $\bar{I}_n$ can be determined not only from the difference between the I_{n+1} and I_n data frames, but can also be predicted from the past 2κ samples of $\bar{I}_n$ as shown in Eqs. (3)–(6). Thus for $2\kappa \le n \le N-2$, and assuming that the previously mentioned conditions are satisfied, we can write

$$\bar{I}_n = D_n = \sum_{l=1}^{2\kappa} a_l\bar{I}_{n-l}; \qquad n = 2\kappa, 2\kappa+1, \ldots, N-2. \tag{7}$$

The Z transform of $\bar{I}_n$ in Eq. (7) gives

$$\bar{I}(z) = \sum_{l=1}^{2\kappa} a_l z^{-l}\bar{I}(z). \tag{8}$$

Equation (8) can be rewritten as

$$\underbrace{\left(\sum_{l=0}^{2\kappa} b_l z^{-l}\right)}_{P(z)}\bar{I}(z) = 0, \tag{9}$$

where $b_l = -a_l$ and $b_0 = 1$. Note that $P(z)$ in Eq. (9) has 2κ complex conjugate roots, let us say $z_k = \exp(jk\alpha)$ and $z_k^* = \exp(-jk\alpha)$ for $k = 1, 2, \ldots, \kappa$. Hence the polynomial $P(z)$ can be expressed as

$$\begin{aligned} P(z) &= \prod_{k=1}^{\kappa} (1 - z_k z^{-1})(1 - z_k^* z^{-1}) \\ &= \prod_{k=1}^{\kappa} \left[z^{-2}(z_k z_k^*) - z^{-1}(z_k + z_k^*) + 1 \right] \\ &= \prod_{k=1}^{\kappa} \left[z^{-2} - 2\cos(k\alpha) z^{-1} + 1 \right]. \end{aligned} \tag{10}$$

Comparing the coefficients of Eqs. (9) and (10), we can write

$$\mathbf{b} = \mathbf{Q}\mathbf{s}, \tag{11}$$

where $\mathbf{b} = [b_0, b_1, b_2, \ldots, b_k, \ldots, b_{2\kappa}]^T$; $\mathbf{Q}$ is the frequency coefficient matrix, $\mathbf{Q} \in \Re^{(2\kappa+1)[\kappa(\kappa+1)/2+1]}$ and $\mathbf{s}$ is the frequency matrix given by Ref. 16:

$$\mathbf{s} = \left[\cos^{\kappa(\kappa+1)/2}(\alpha) \quad \cos^{\kappa(\kappa+1)/2-1}(\alpha), \ \ldots, \ \cos(\alpha) \ 1 \right]^T$$

of size

$$\left[\frac{\kappa(\kappa+1)}{2} + 1 \right] \times 1.$$

Thus the design of the matrices $\mathbf{Q}$ and $\mathbf{b}$ yields the matrix $\mathbf{s}$ from which the phase step α can be subsequently computed. The design of the matrix $\mathbf{Q}$ will be explained in Section 3. Assuming that the matrix $\mathbf{Q}$ is known the matrix $\mathbf{b}$ can be computed by observing that the multiplication in the frequency domain is equivalent to a convolution in the time domain. Hence Eq. (9) in the time domain can be written as

$$\bar{\mathbf{I}}_n \otimes \mathbf{b} = 0, \tag{12}$$

where $\bar{\mathbf{I}}_n = [\bar{I}_n, \bar{I}_{n-1}, \bar{I}_{n-2}, \ldots, \bar{I}_{n-\kappa}, \ldots, \bar{I}_{n-2\kappa}]^T$. Equation (12) can be further written as

$$\bar{\mathbf{I}}_n{}^T \mathbf{b} = 0 \quad n \geq 2\kappa,$$

$$\bar{\mathbf{I}}_n{}^T \mathbf{Q}\mathbf{s} = 0 \quad n \geq 2\kappa. \tag{13}$$

Finally, in the ideal case, the phase step α can be obtained by solving Eq. (13).

Since the additive random noise influences the measurement, the intensity I_n, at the nth data frame, in the presence of noise can be written as

$$\hat{I}_n = I_n + \eta_n \quad n = 0, \ 1, \ 2, \ \ldots, \ N-1, \tag{14}$$

where η_n is the white Gaussian random noise with mean zero and variance σ^2. Let $\mathbf{I}_n''$ denote matrix $\bar{\mathbf{I}}_n$ in the presence of noise. In this case, the convolution of vectors $\mathbf{I}_n''$ and $\mathbf{b}$ in Eq. (12) rather than yielding zero will give an error e_n:

$$\begin{aligned} e_n &= \mathbf{I}_n'' \mathbf{b}; \quad \text{for } n = 2\kappa, \ 2\kappa+1, \ 2\kappa+2, \ \ldots, \ N-2 \\ &= \mathbf{I}_n'' \mathbf{Q}\mathbf{s}. \end{aligned} \tag{15}$$

Representing all the $(N - 2\kappa - 2)$ prediction errors $\{e_n\}$ in a vector form, we have

$$\mathbf{e} = \mathbf{I}'' \mathbf{Q}\mathbf{s}, \tag{16}$$

where $\mathbf{e}$ is the error vector and $\mathbf{I}'' = [\mathbf{I}_{N-2}'', \mathbf{I}_{N-3}'', \ldots, \mathbf{I}_{2\kappa}'']^T$.

Finally, in the presence of noise the phase step α can be estimated, let us say $\hat{\alpha}$ by minimizing the error vector $\mathbf{e}$ in Eq. (16). We apply the least-squares approach to estimate the phase step α. We minimize the cost function given by

$$\Psi(\alpha) = \mathbf{e}^T \mathbf{e} \tag{17}$$

to yield $\hat{\alpha}$. This is done by equating the derivative of $\Psi(\alpha)$ with respect to α to zero:

$$\frac{\partial \Psi(\alpha)}{\partial \cos(\alpha)} = 0 \Rightarrow \mathrm{tr}\left[\frac{\partial \mathbf{e}^T \mathbf{e}}{\partial \cos(\alpha)} \right] = 0,$$

$$\text{i.e., } \mathrm{tr}\left[\frac{\partial (\mathbf{s}^T \mathbf{s})}{\partial \cos(\alpha)} \mathbf{Q}^T (\mathbf{I}'')^T \mathbf{I}'' \mathbf{Q} \right] = 0, \tag{18}$$

where "tr" denotes the trace operation. The trace in Eq. (18) can be minimized by using any standard global or local search algorithm. We will discuss the application of the proposed method in the estimation of phase step values and the subsequent determination of the phase distribution in Section 3.

3. Evaluation of the Algorithm

The proposed concept is tested by simulating the fringe pattern in Eq. (1), and the phase step is arbitrarily selected as $\alpha = 41.8°$. We will study this for $\kappa = 1$ and $\kappa = 2$. The minimum number of data frames required for retrieving the phase steps is twice the number of frequencies present in the signal. However, the presence of random noise necessitates acquiring additional data frames. During the simulation, additive white Gaussian noise is added to the fringe pattern in Eq. (1) and the signal-to-noise ratio (SNR) is varied from 10 to 80 dB in steps of 0.1 dB. The first step during the implementation of the proposed concept involves identifying the order of harmonics present in the acquired data. Although determining the order of harmonics is a standard problem in classical signal processing,[20] we will for the sake of simplicity assume here that we have *a priori* knowledge about the order of harmonics. The second step involves the design of a polynomial in Eq. (10). For $\kappa = 1$ the polynomial $P(z)$ is

$$P(z) = z^{-2} - 2\cos(\alpha) z^{-1} + 1. \tag{19}$$

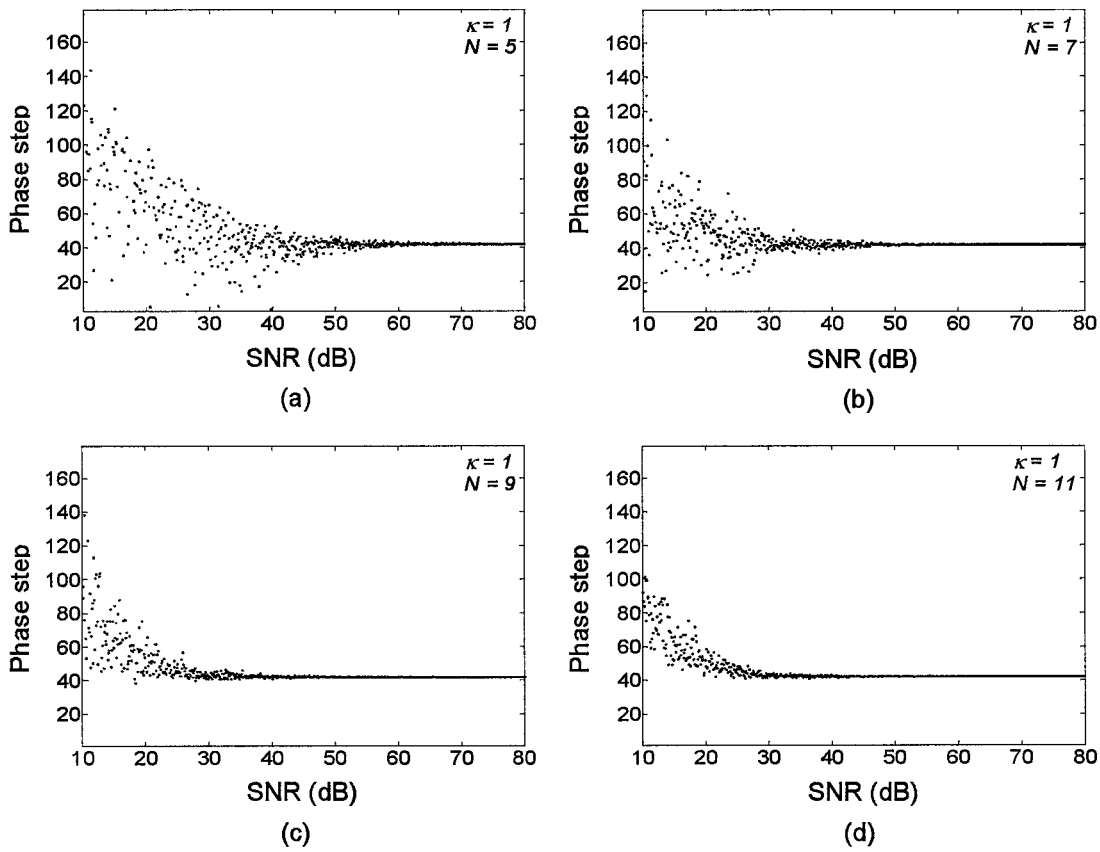

Fig. 1. Plots of phase step α (in degrees) versus SNR obtained using Eq. (18) at an arbitrary pixel point on a data frame for κ = 1 and $N = 5, 7, 9$, and 11, respectively.

Comparing the coefficients of z^{-1} in Eq. (19) with the coefficients of z^{-1} in Eq. (9) we obtain

$$b_0 = b_2 = 1,$$
$$b_1 = -2\cos(\alpha). \tag{20}$$

Hence the matrices **b**, **Q** and, **s** in Eq. (11) can be written as

$$\underbrace{\begin{pmatrix} b_2 \\ b_1 \\ b_0 \end{pmatrix}}_{\mathbf{b}} = \underbrace{\begin{pmatrix} 0 & 1 \\ -2 & 0 \\ 0 & 1 \end{pmatrix}}_{\mathbf{Q}} \underbrace{\begin{pmatrix} \cos(\alpha) \\ 1 \end{pmatrix}}_{\mathbf{s}}. \tag{21}$$

The knowledge of matrices **Q** and **s** allows for determining the error vector **e** in Eq. (16). The cost function in Eq. (18) is then minimized to estimate the values of the phase steps. We chose a global search algorithm (PGSL) for performing the minimization in Eq. (18). For details on the algorithm the reader is referred to Ref. 21.

Figures 1(a)–1(d) show the influence of the number of data frames on the estimation of the phase steps. Figure 1 shows that as the number of data frames increases, the reliability in the estimation of phase step values at low SNRs is also increased. For instance, Fig. 1(b) shows that the phase steps can be estimated within an allowable error for SNR = 50 dB and above as compared for SNR = 60 dB and above in Fig. 1(a). Similarly, Fig. 1(d) shows that the phase steps can be estimated for SNR = 30 dB onwards as compared with SNR = 40 dB onwards in Fig. 1(c).

Let us now consider the case when κ = 2 in Eq. (1). The polynomial $P(z)$ in Eq. (10) is

$$\begin{aligned} P(z) &= \prod_{k=1}^{2}\left[z^{-2} - 2\cos(k\alpha)z^{-1} + 1\right] \\ &= \left[z^{-2} - 2z^{-1}\cos(\alpha) + 1\right]\left[z^{-2} - 2\cos(2\alpha)z^{-1} + 1\right]. \end{aligned} \tag{22}$$

Simplifying Eq. (22) and comparing it with the coefficients of z^{-1} in Eq. (9) gives

$$b_0 = b_4 = 1,$$
$$b_1 = b_3 = 8\cos^3(\alpha) - 4\cos(\alpha) + 2,$$
$$b_2 = -4\cos^2(\alpha) - 2\cos(\alpha) + 2. \tag{23}$$

Equation (11) could then be written as

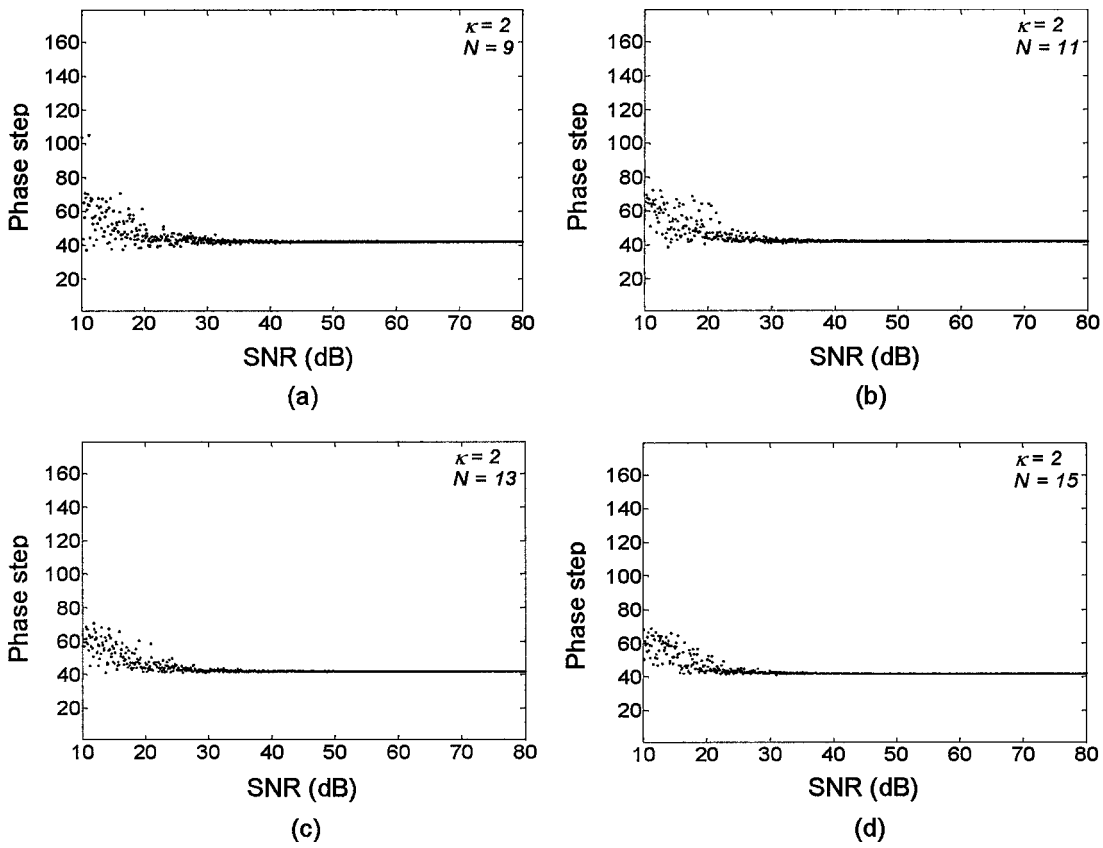

Fig. 2. Plots of phase step α (in degrees) versus SNR obtained using Eq. (18) at an arbitrary pixel location on a data frame for κ = 2 and $N = 9$, 11, 13, and 15, respectively.

$$\underbrace{\begin{pmatrix} b_4 \\ b_3 \\ b_2 \\ b_1 \\ b_0 \end{pmatrix}}_{\mathbf{b}} = \underbrace{\begin{pmatrix} 0 & 0 & 0 & 1 \\ 0 & -4 & -2 & 2 \\ 8 & 0 & -4 & 2 \\ 0 & -4 & -2 & 2 \\ 0 & 0 & 0 & 1 \end{pmatrix}}_{\mathbf{Q}} \underbrace{\begin{pmatrix} \cos^3(\alpha) \\ \cos^2(\alpha) \\ \cos(\alpha) \\ 1 \end{pmatrix}}_{\mathbf{s}}. \quad (24)$$

A procedure similar to that described for the single harmonic case is followed for the estimation of phase steps. Figures 2(a)–2(d) show the influence of the increase in the number of data frames on the determination of the values of the phase steps. Figure 2(d) shows that phase steps can be estimated for SNR = 25 dB onwards as compared to SNR = 30 dB on-

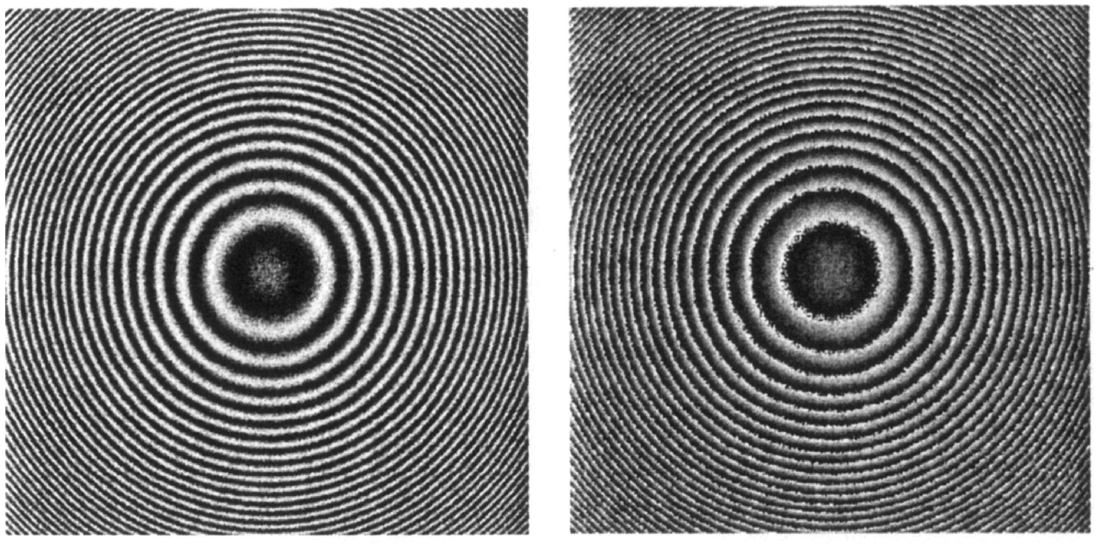

Fig. 3. (a) Fringe pattern and (b) wrapped phase distribution φ.

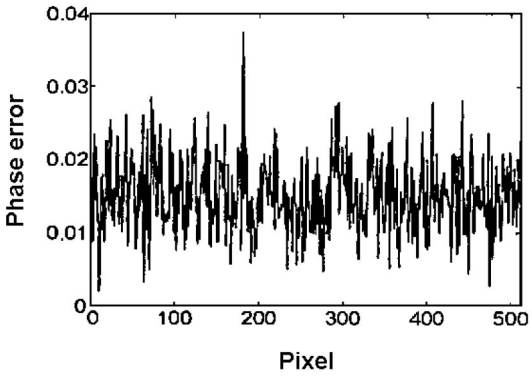

Fig. 4. Plot of typical phase errors (in radians) in the computation of phase distribution φ corresponding to the phase step obtained from Fig. 1(d) for SNR = 30 dB.

wards in Fig. 2(c). Obviously, the number of data frames is increased in the present case as compared to the case when $\kappa = 1$. The number of data frames used during the present simulations is $N = 9, 11, 13$, and 15.

Once the phase step values have been estimated, phase φ in Eq. (1) can be computed by using the least-squares approximation method.[17,18] Figure 3(b) shows the wrapped phase for a simulated fringe map in Fig. 3(a). Figure 4 shows typical errors occurring during the estimation of phase φ at SNR = 30 dB and for the phase step value obtained from Fig. 1(d).

4. Comparison and Discussion

The proposed method is further compared with respect to other well-known conventional algorithms[13,15,22,23] to test its efficiency in estimating the phase in the presence of noise. The comparison is performed in an objective manner by selecting only those phase steps for which these algorithms have been designed. It is important to note that in our proposed method the selection of arbitrary phase steps between the data frames is possible. We did not find it necessary to compare the algorithms proposed by Carré[1] and Hariharan[10] with our method since these algorithms cannot handle the presence of multiple-order harmonics in the wavefront. Figure 5 shows the plots of the mean-squared error (MSE) of the phase computed at different SNRs and for various values of linear miscalibration error ε in the phase step α. During the comparison, we considered for our method seven data frames, and we performed 100 Monte Carlo simulations at each SNR value. Figure 5(a) shows that for zero miscalibration error, $\varepsilon = 0.0\%$, the conventional algorithms performed better than our method. Unfortunately, there is always some magnitude of linear miscalibration error asso-

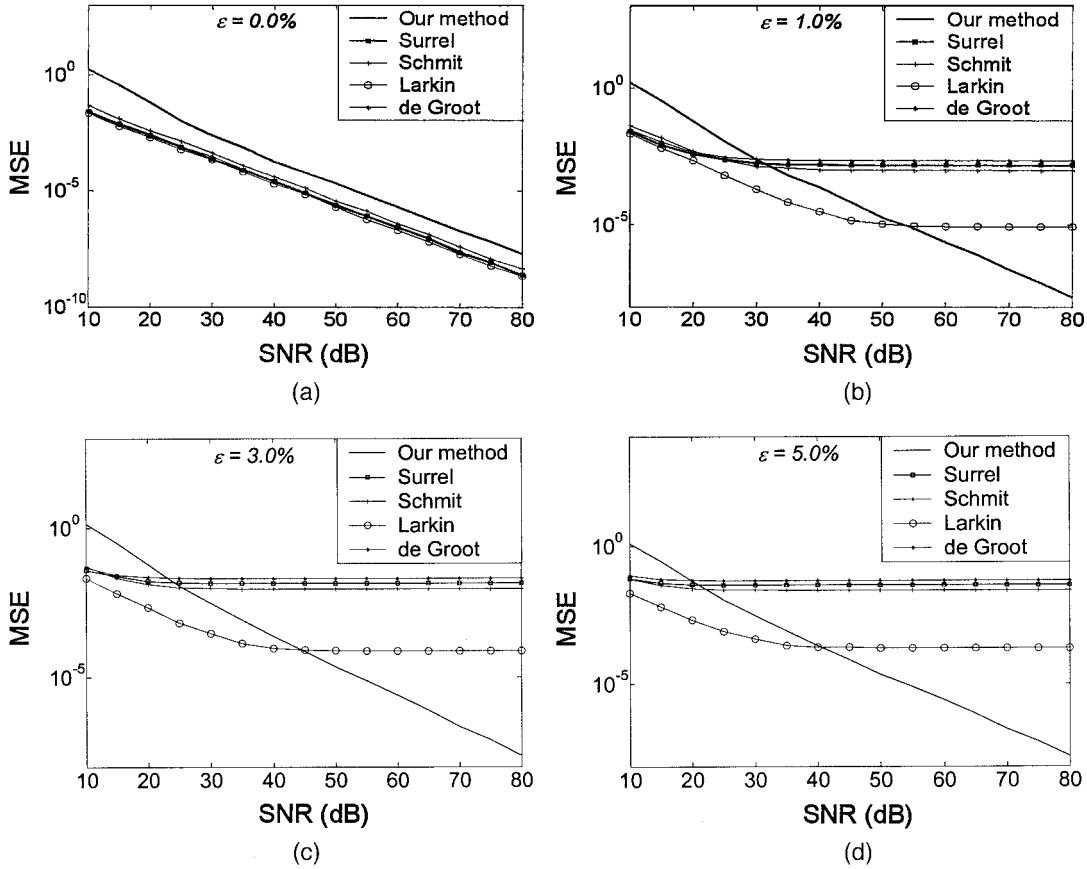

Fig. 5. Comparison of our method with the algorithms developed by Surrel, Schmit, Larkin, and de Groot for the computation of phase φ for different values of linear miscalibration errors ε; (a) 0.0%, (b) 1.0%, (c) 3.0%, and (d) 5.0%. Y axis represents the MSE (in radians^2).

ciated with the PZT, and hence exactness of the desired phase step is not guaranteed. Figures 5(b)–5(d) show the plots of MSE for different miscalibration errors. The plots show that as the miscalibration error increases all the standard algorithms tend to have a constant MSE in the computation of phase φ, irrespective of an increase in the SNR. Our method, however, exhibits a decrease in the MSE as the SNR increases. These comparisons, when extended to higher-order harmonics, yield similar results. A noteworthy point associated with our method is that it has the potential to work efficiently even in the presence of any order detector nonlinearity.[24] Our method will produce still better results if a greater number of data frames are acquired. Moreover, this linear prediction approach can be extended to optical configurations consisting of multiple PZTs. The concept of multiple PZTs in an optical setup was first proposed by Rastogi[25] for determining two orthogonal displacement components simultaneously. In such cases, these conventional algorithms cannot be adapted to accommodate dual PZTs.

5. Conclusions

We have presented a novel approach for predicting the phase step values pixelwise in the presence of linear miscalibration errors, harmonics, and noise. Our method can also compensate for detector nonlinearity. The study shows that as the number of data frames increase, the phase steps can be estimated at lower SNRs. A comparison with several benchmarking algorithms shows the feasibility of our proposed method in the estimation of phase.

This research was partly funded by the Swiss National Science Foundation.

References

1. P. Carré, "Installation et utilisation du comparateur photoélectrique et interférentiel du Bureau International des Poids et Mesures," Metrologia **2,** 13–23 (1966).
2. J. H. Bruning, D. R. Herriott, J. E. Gallagher, D. P. Rosenfeld, A. D. White, and D. J. Brangaccio, "Digital wavefront measuring interferometer for testing optical surfaces and lenses," Appl. Opt. **13,** 2693–2703 (1974).
3. K. Creath, "Phase-shifting holographic interferometry," in *Holographic Interferometry,* P. K. Rastogi, ed., Vol. 68 of Optical Sciences Series (Springer, 1994), pp. 109–150.
4. T. Kreis, *Holographic Interferometry Principles and Methods* (Akademie Verlag, 1996), pp. 101–170.
5. J. E. Greivenkamp and J. H. Bruning, "Phase shifting interferometry," in *Optical Shop Testing,* D. Malacara, ed. (Wiley, 1992), pp. 501–598.
6. G. T. Reid, "Automatic fringe pattern analysis: a review," Opt. Lasers Eng. **7,** 37–68 (1986).
7. G. Stoilov and T. Dragastinov, "Phase-stepping interferometry: five-frame algorithm with an arbitrary step," Opt. Lasers Eng. **28,** 61–69 (1997).
8. J. Schwider, R. Burow, K. E. Elssner, J. Grzanna, R. Spolaczyk, and K. Merkel, "Digital wave-front measuring interferometry: some systematic error sources," Appl. Opt. **22,** 3421–3432 (1983).
9. Y. Zhu and T. Gemma, "Method for designing error-compensating phase-calculation algorithms for phase-shifting interferometry," Appl. Opt. **40,** 4540–4546 (2001).
10. P. Hariharan, B. F. Oreb, and T. Eiju, "Digital phase-shifting interferometry: a simple error-compensating phase calculation algorithm," Appl. Opt. **26,** 2504–2506 (1987).
11. J. Schwider, O. Falkenstorfer, H. Schreiber, and A. Zoller, "New compensating four-phase algorithm for phase-shift interferometry," Opt. Eng. **32,** 1883–1885 (1993).
12. Y. Surrel, "Phase stepping: a new self-calibrating algorithm," Appl. Opt. **32,** 3598–3600 (1993).
13. Y. Surrel, "Design of algorithms for phase measurements by the use of phase stepping," Appl. Opt. **35,** 51–60 (1996).
14. K. Hibino, B. F. Oreb, D. I. Farrant, and K. G. Larkin, "Phase shifting for nonsinusoidal waveforms with phase-shift errors," J. Opt. Soc. Am. A **12,** 761–768 (1995).
15. K. G. Larkin and B. F. Oreb, "Design and assessment of symmetrical phase-shifting algorithms," J. Opt. Soc. Am. A **9,** 1740–1748 (1992).
16. K. W. Chan and H. C. So, "Accurate frequency estimation for real harmonic sinusoids," IEEE Signal Process. Lett. **7,** 609–612 (2004).
17. C. J. Morgan, "Least-squares estimation in phase-measurement interferometry," Opt. Lett. **7,** 368–370 (1982).
18. J. E. Greivenkamp, "Generalized data reduction for heterodyne interferometry," Opt. Eng. **23,** 350–352 (1984).
19. C. Rathjen, "Statistical properties of phase-shift algorithms," J. Opt. Soc. Am. A **12,** 1997–2008 (1995).
20. J. J. Fuchs, "Estimating the number of sinusoids in additive white noise," IEEE Trans. Acoust., Speech, Signal Process. **36,** 1846–1853 (1988).
21. B. Raphael and I. F. C. Smith, "A direct stochastic algorithm for global search," App. Math. Comput. **146,** 729–758 (2003).
22. J. Schmit and K. Creath, "Some new error-compensating algorithms for phase- shifting interferometry," *Optical Fabrication and Testing Workshop,* Vol. 13 of 1994 OSA Technical Digest Series (Optical Society of America, 1994), p. PD-4.
23. P. de Groot, "Long-wavelength laser diode interferometer for surface flatness measurement," in *Optical Measurements and Sensors for the Process Industries,* C. Gorecki and R. W. Preater, eds., Proceedings of the Society of Photo-Optical Instrument Engineers (1994), Vol. 2248, pp. 136–140.
24. J. Schmit and K. Creath, "Extended averaging technique for derivation of error-compensating algorithms in phase shifting interferometry," Appl. Opt. **34,** 3610–3619 (1995).
25. P. K. Rastogi, "Phase shifting applied to four-wave holographic interferometers," Appl. Opt. **31,** 1680–1681 (1992).